

## Developing Soil Models for Dynamic Impact Simulations

Edwin L. Fasanella  
[Edwin.L.Fasanella@nasa.gov](mailto:Edwin.L.Fasanella@nasa.gov)

Karen H. Lyle  
[Karen.H.Lyle@nasa.gov](mailto:Karen.H.Lyle@nasa.gov) [Karen.E.Jackson-1@nasa.gov](mailto:Karen.E.Jackson-1@nasa.gov)

Karen E. Jackson

Mail Stop 495  
NASA Langley Research Center  
Hampton, VA 23681

### ABSTRACT

This paper describes fundamental soils characterization work performed at NASA Langley Research Center in support of the Subsonic Rotary Wing (SRW) Aeronautics Program and the Orion Landing System (LS) Advanced Development Program (ADP). LS-DYNA<sup>®</sup><sup>1</sup> soil impact model development and test-analysis correlation results are presented for: (1) a 38-ft/s vertical drop test of a composite fuselage section, outfitted with four blocks of deployable energy absorbers (DEA), onto sand, and (2) a series of impact tests of a 1/2-scale geometric boilerplate Orion capsule onto soil. In addition, the paper will discuss LS-DYNA contact analysis at the soil/structure interface, methods used to estimate frictional forces, and the sensitivity of the model to density, moisture, and compaction.

### INTRODUCTION

Since its inception in 2006, the NASA Subsonic Rotary Wing (SRW) Aeronautics Program in Rotorcraft Crashworthiness has focused attention on improved prediction of rotorcraft crashworthiness. Several research topics have been identified to achieve this goal, including: fundamental materials characterization, human occupant modeling and injury prediction, development of system integrated simulation models, model validation studies that focus on probabilistic analysis and uncertainty quantification, and multi-terrain impact simulation [1]. Multi-terrain impact simulations are important since over 85 percent of helicopter crash impacts occur on unprepared surfaces.

Along a separate path, the Orion Landing System (LS) Advanced Development Program (ADP) has been investigating landing of the Orion space capsule onto land and water [2]. After retiring the Space Shuttle in 2010, NASA plans to replace the human access to space with the Orion spacecraft, a capsule that is larger than the Apollo command module with room for up to six astronauts. The Orion capsule will service the International Space Station (ISS), and later versions are planned to travel to the moon and then on to Mars. On return from space, the Orion capsule will descend to earth suspended from parachutes. Weight constraints are steering the current Orion design towards water landings, but a design goal was established for the Orion crew to “walk away” from land landings due to a pad abort or for any other contingency land landing. Landing site terrain is highly variable, with very hard soil at sites such as the dry-lake beds in California near NASA Dryden and very soft soil at sites such as Carson Sink, Nevada. For a pad or ascent abort from NASA Kennedy Space Center (KSC), water is the preferred

<sup>1</sup> Trade names and trademarks are used in this report for identification only. Their usage does not constitute an official endorsement, either expressed or implied, by the National Aeronautics and Space Administration.

impact surface. However, if the capsule blows back onto land, the impact surface can vary from extremely soft dry sand to hard prepared surfaces near the pad. Consequently, landing systems for Orion must be designed for multi-terrain impacts. A team of NASA engineers and soil scientists visited the potential western sites, as well as KSC and Langley, to make in-situ measurements of the soils and to gather soil samples for laboratory analysis.

This paper will take advantage of fundamental soils characterization work performed for both programs and will present results of LS-DYNA® [3] soil models and simulations, and test-analysis correlation conducted for the Orion LS ADP and for the NASA SRW crashworthiness program. In addition, the paper will discuss LS-DYNA contact analysis at the soil/structure interface, methods used to estimate frictional forces, and the sensitivity of the model to density, moisture, and compaction. Although both Lagrangian and Eulerian formulations were developed for soil models; the Eulerian model was found to require a longer run time to produce comparable results, and the effects of friction were not easily determined. Thus, results reported in the present paper were executed using a Lagrangian soil model.

## **SOILS CHARACTERIZATION**

Ten Mat 5 (MAT\_SOIL\_AND\_FOAM) soil models were generated for LS-DYNA by Applied Research Associates, Inc. (ARA) [4-6]. Soil samples that were collected in-situ and tested in the ARA laboratory varied from the hard-clay at the Cuddeback dry lake bed in California near NASA Dryden to the soft dry sand from dunes at KSC in Florida. Mat 5 soil models are robust and relatively simple to construct. When the shear failure surface (strength) is exceeded, the deviatoric stresses are limited by the failure surface and the material can then flow like a viscous fluid. The strength of the soil is pressure dependent in the Mat 5 models. Soft soils such as sand must be confined to prevent flowing under gravitational loads. Gravitational loads are required in the simulations to produce a pressure gradient with soil depth. Two different sands, one clean and one mixed with clay that were used for impact surfaces at NASA Langley, were characterized. Soils and many geomaterials typically fail in shear. Testing to determine the shear failure envelope, which depends on the confining pressure, is generally accomplished in the laboratory using a strength test called the tri-axial compression test (ASTM standard D4767-04). Moisture content is quite important, especially for clays where the absorbed moisture forms a thin film over each minute clay particle. The moisture film allows the clay particles to slide over each other and can drastically reduce the shear strength. Also, as water builds up between the soil particles or grains, a “pore” pressure is developed that reduces the shear strength. The shear strength of sand is not affected as adversely with moisture since sand particles are larger and do not absorb water. Also, in contrast to clays, water tends to drain from sand quite rapidly. The moisture content is calculated to be the weight of the water in the soil divided by the weight of the dried soil, and it should be recorded. The moisture content and density of the in-situ soil must be known, as the soil behavior is highly dependent on both. The effect of pore pressure, which is highly dynamic, is not accounted for in the Mat 5 model. Consequently, dynamic models for clay and silts with high moisture content may not always give good results. Further details on soils testing and analysis are described in the following sections.

### ***Tri-axial Compression Test Apparatus***

The tri-axial test apparatus can be used for strength testing of soils, compressibility testing, and can be used to determine bulk unloading modulus by a hydrostatic compression test where the soil is loaded to the same pressure on all surfaces. Schematic drawings and a picture of the tri-axial compression test apparatus that is used to determine constitutive properties of a soil in a commercial testing laboratory are shown in Figures 1 and 2 [4]. A cylinder with the soil sample “reconstituted” as nearly as possible to the in-situ density and moisture is enclosed within a fluid-tight membrane.

### ***Strength Testing***

To determine shear strength, i.e., the yield surface, a series of axial compression tests are conducted. In the test series, the side-wall confining pressure, which is produced on the membrane using compressed air, is incremented. The sidewall confining pressure represents the pressure of the adjacent soil in the field. The increment of axial stress above the confining pressure (stress difference) results in shear stresses on all planes except the principal directions parallel and perpendicular to the specimen axes. The data are manipulated to fit the shear failure criteria in Mat 5; which has a quadratic pressure dependent failure strength of the form  $a_0 + a_1p + a_2p^2$ , where the a’s are coefficients determined from the tri-axial test and “p” is the mean stress. The equations of the a-coefficients are derived later in this section. Note that due to gravity, confining pressure increases with soil depth, so the lower pressures correspond to the upper soil. If the shear strength of a material is very low as for dry sand, the Mat 5 model gives fluid-like behavior.

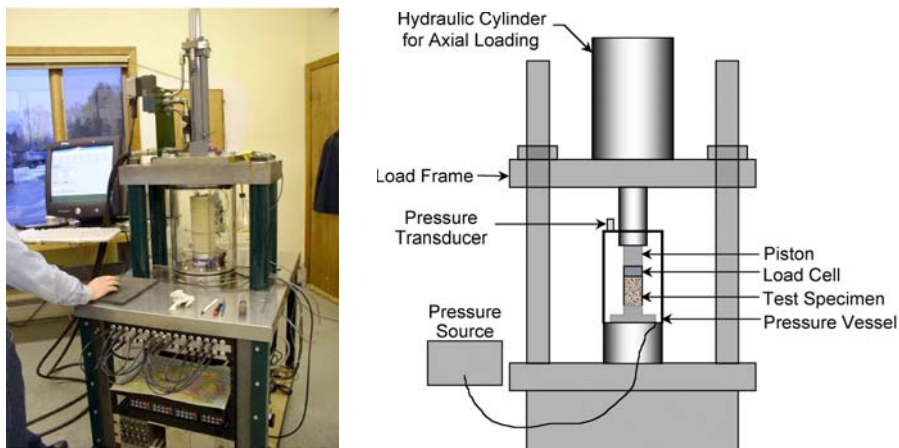


Figure 1. Picture and schematic of tri-axial compression test for soil characterization.

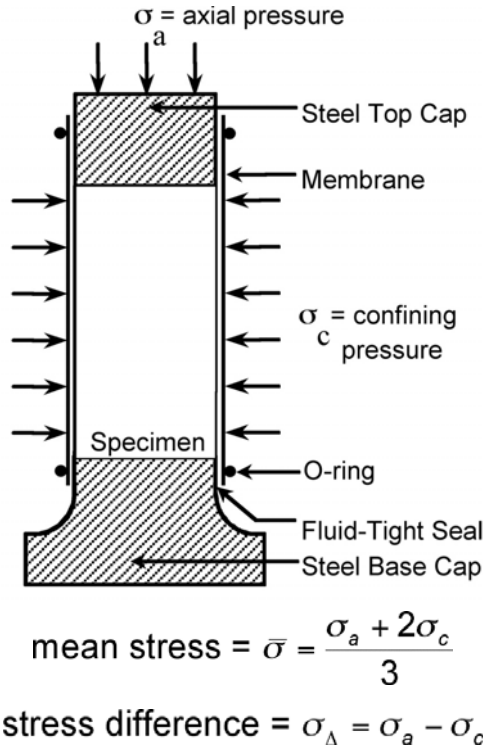


Figure 2. Schematic of tri-axial compression test with equations for mean stress and stress difference.

***Derivation of Shear Failure Surface for Mat 5 Model***

In the tri-axial compression test, for a given confining pressure,  $\sigma_c$ , the maximum stress difference is determined when the soil yields due to shear. The stress difference is the difference between the true axial stress,  $\sigma_a$ , and the true radial or confining stress,  $\sigma_c$ . The tri-axial test is typically run for 3 to 5 increasing confining pressures and the data is plotted with the mean stress, which is  $p$ , on the X-axis and the stress difference on the Y-axis. This plot provides the shear strength envelope or yield surface of the material from which the values of  $a_0$ ,  $a_1$ , and  $a_2$  can be determined. From the LS-DYNA theory manual [7], the pressure dependent shear strength envelope is written in terms of a quadratic in pressure by the equation:

$$1/2s_{ij}s_{ij} = (a_0 + a_1p + a_2 p^2) \tag{Eq. 1}$$

where  $p$  is the mean pressure,  $s_{ij}$  is the deviatoric stress tensor, and the “a” coefficients are determined from the tri-axial compression tests. The left hand portion of Equation 1 is the stress invariant  $J_2'$  associated with shear. By expanding the stress tensor, it can be shown that:

$$J_2' = 1/3 (\sigma_c - \sigma_a)^2 = 1/3 \sigma_D^2 \tag{Eq. 2}$$

Consequently, a linear fit of mean stress,  $p$ , versus the stress difference,  $\sigma_D$ , gives a form

$$\sigma_D = mp + C \tag{Eq. 3}$$

where  $m$  is the slope of the line and  $C$  is the Y-intercept. The Y-intercept is known as the cohesion of the soil. If the cohesion is small, as it is for dry sand, then  $C=0$ . Next by squaring Equation 3:

$$1/3 \sigma_D^2 = (1/3m^2)p^2 + (2/3mC)p + 1/3C^2 = a_0 + a_1p + a_2 p^2 \quad (\text{Eq. 4})$$

The coefficients  $a_0$ ,  $a_1$ , and  $a_2$  are found by equating the coefficients in Equation 4. For the case of  $C=0$ , then  $a_2$  is the only remaining term and is equal to  $1/3$  the square of the slope of the mean stress versus stress difference curve.

Other material models for soils in LS-DYNA with pressure dependence include the Mat25 Geological Cap model. The “Cap” model is more complex than Mat 5 as it uses two surfaces instead of one, an initial yield surface and a failure surface. The Mat 5 model is considered well suited for preliminary design purposes. However, the two-surface Cap model is a higher fidelity model that should be considered for severe dynamic conditions.

### ***Compressibility testing***

A series of uni-axial tests can be conducted using the tri-axial apparatus so that the confining pressure is adjusted as the axial pressure is increased to produce no radial strain. Since the axial strain is different from the radial strain, shear stresses develop, but shear failure does not occur. From the uni-axial test, compressibility in the form of pressure versus natural (logarithmic) volumetric strain can be calculated for input into the Mat 5 model. (Axial strain is equal to volumetric strain since the radial strain is zero.) Up to 10 pairs of data are allowed. Also, from the plot of axial stress versus confining pressure, Poisson’s ratio can be calculated. Other constants such as  $G$ , the shear modulus, can also be calculated from this test or from the hydrostatic compression test, which will be discussed next.

### ***Hydrostatic Compression***

Hydrostatic compression tests can also be conducted using the tri-axial compression apparatus. For these tests, the soil sample is loaded only by air. Consequently, the pressure on the specimen is the same in all directions and no shear stress develops. These tests can be used to define volumetric strain versus pressure for the Mat 5 model. The initial slope of the curve is the bulk loading modulus  $K_L$  and the unloading curve can be used to determine the unloading bulk modulus  $K_u$  for Mat 5. Also, the shear modulus,  $G$ , can be obtained from Eq. 6 below. With  $G$  determined, one now has enough information for the Mat 5 material model.

Recall that:

$$K_L = E/3(1-2\nu) \quad (\text{Eq. 5})$$

$$\text{and } G = E/2(1+\nu) = 3/2 K_L(1-2\nu)/(1+\nu) \quad (\text{Eq. 6})$$

## LS-DYNA SIMULATIONS

LS-DYNA simulations were performed to simulate: (1) a 38-ft/s vertical drop test of a composite fuselage section, outfitted with four blocks of deployable energy absorbers (DEA), onto sand, and (2) a series of impact tests of a ½-scale geometric boilerplate Orion capsule onto soil. Each test, along with LS-DYNA [3] simulations, will be presented in the following sections of the paper.

### *Fuselage Section Drop Test Into Sand and LS-DYNA Simulation*

LS-DYNA simulations were performed as part of the SRW Program for a vertical drop test onto soft clean sand of a 5-ft. diameter, 5-ft. long composite fuselage section that was retrofitted with an externally deployable energy absorber (DEA) concept. Detailed finite element models were developed to represent the fuselage section, the DEA, and the soft soil. The models were executed in LS-DYNA and analytical predictions were correlated with test data. The level of agreement is dependent on accurately modeling the behavior of the soil, which can be highly variable depending on moisture content, texture, and density. Following the impact test, a penetrometer, instrumented with a tri-axial accelerometer, was dropped multiple times to characterize the variability of the soft soil.

Prior to the test, ten 100-lb lead blocks were attached to the floor of the fuselage section through standard seat rails, five blocks per side. The fuselage section was instrumented with accelerometers (250-G maximum range) to record the structural response of the floor. Pre- and post-test photographs of the test article are shown in Figure 3. A 12-ft x 12-ft wooden box filled to a height of 2 ½-ft with high-grade “washed” sand was installed beneath the drop tower at NASA Langley. More details on the construction of the fuselage section can be found in Reference 8.

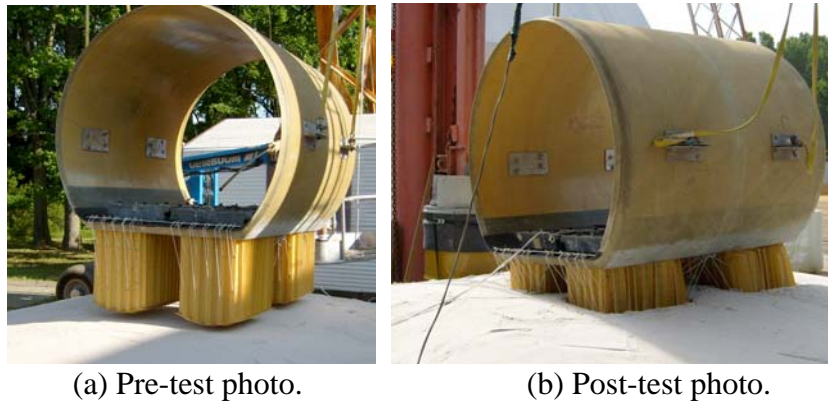


Figure 3. Photographs from the drop test onto sand.

The DEA is an expandable honeycomb structure designed to absorb impact energy by crushing. The concept is based on a patented flexible hinge at each junction of its cell walls. This feature enables almost any size and strength energy absorber to be fabricated and readily deployed. Like conventional honeycomb, once expanded, the energy absorber is transformed into an efficient orthotropic cellular structure, with greater stiffness and strength along the cell axis as compared to the transverse directions. The flexible hinge enables various methods of expanding the

cellular structure. Four blocks of DEA were mounted to the bottom of the floor of the composite fuselage section, as shown in Figure 3(a). Each block had dimensions of 20-in. high, 20.5-in. deep, and 16.5-in. wide. The bottom surface of the DEA blocks was curved (radius 18-in.) to reduce peak loads during initial impact. A single layer of Kevlar fabric was used to cover the bottom, curved surface of each DEA block to ensure proper load transfer into the cell walls. Additional information regarding the development and testing of the DEA can be found in References 9 and 10.

Pre-test predictions of the soft soil (sand) impact test were generated in LS-DYNA initially using a Mat 63 material model to represent the soil, as documented in Reference 11. Mat 63 is typically used to represent crushable foams in LS-DYNA. Test-analysis correlation results indicated that the Mat 63 model retains too much elastic energy, which is released to produce excessive rebound. Another shortcoming of the Mat 63 model is that the unloading curve cannot be specified independently, and Poisson's ratio is effectively zero. A soft soil may initially load with a relatively small modulus, while the unloading may require a very large unloading modulus. The tension cutoff must be nonzero to prevent element failure under small element strains. Consequently, other soil models were investigated and the Mat 5 model was chosen for additional analysis due to its simplicity and added flexibility. The Mat 5 model has a shear failure surface that is pressure dependent, which is a basic property of geo-materials, and unlike Mat 63 allows for a separate unloading bulk modulus. In addition, the Mat 5 model is more fluid-like under many conditions, which is ideal for a soft soil. In the Mat 5 material model, the yield surface, i.e., strength of the soil, increases with larger confining pressures.

A picture of the fuselage and sand model is shown in Figure 4. The lead blocks on the floor are represented using 40 concentrated masses. Also, the deployable energy absorbers are modeled using solid elements that are assigned material properties obtained from a dynamic crush test of a deployable energy absorber component. The soil is represented using Mat 5 and the specific material input parameters were partially determined from post-test penetrometer drops.

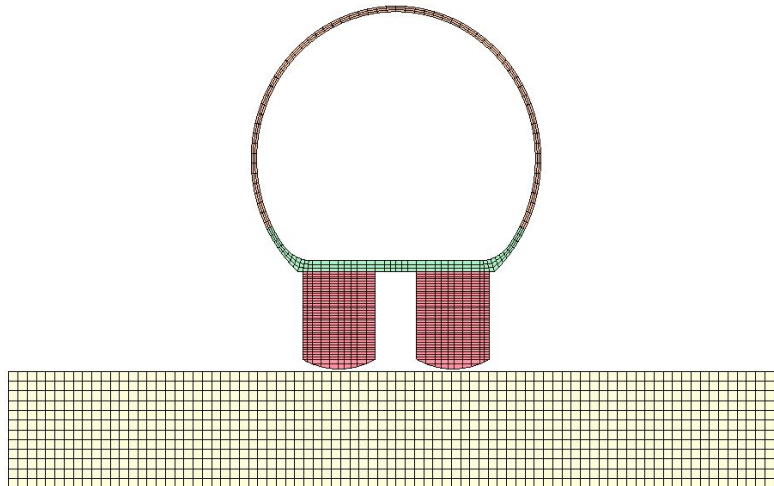
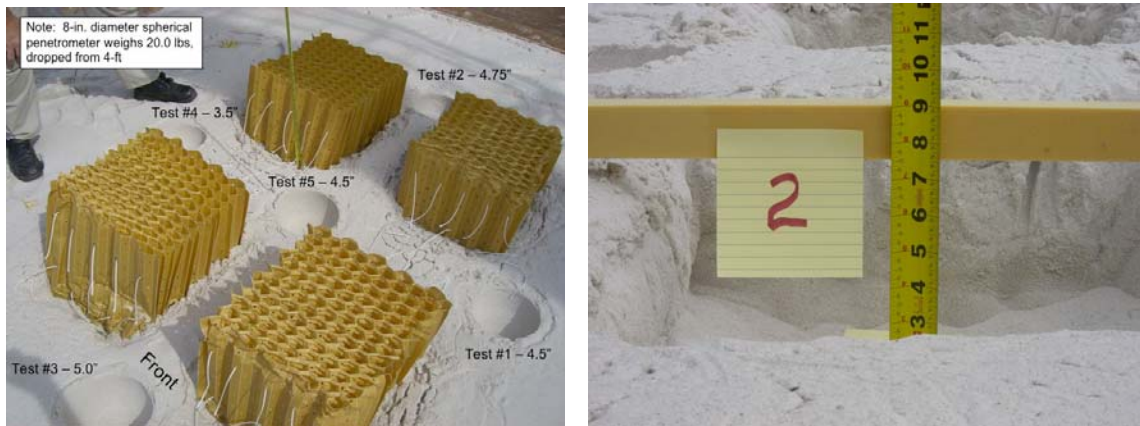


Figure 4. LS-DYNA model of fuselage with DEA above sand.

Following the fuselage section impact test, an 8-in.-diameter penetrometer, which weighed 20 pounds, was dropped at five undisturbed locations to dynamically characterize the material

properties of the sand. The hemispherical penetrometer was instrumented with a tri-axial accelerometer and was dropped from a height of 4-ft onto the sand to produce an impact velocity of approximately 16-ft/s. Knowing the initial conditions, the acceleration response of the penetrometer, and the depth of the resulting impression in the sand, the soil model can be verified. A photograph showing the penetrometer test locations is provided in Figure 5(a).

Following the penetrometer tests, the deployable energy absorbers were removed from the sand and post-test measurements of the depth of the impressions left in the sand were made. A photograph illustrating the measurement technique is shown in Figure 5(b). The maximum crater depths were measured to be from 7.5 to 9 inches. The average crush of each 20-in. high DEA block was also in the same range.



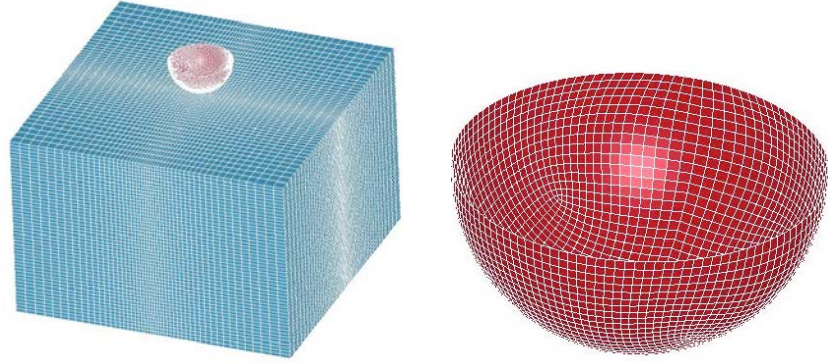
(a) Penetrometer test locations.

(b) Crater depth measurement.

Figure 5. Photographs illustrating post-test measurements.

Accelerometer data and sand penetration depths from the five penetrometer tests, shown in Figure 5, were analyzed. The depth of penetration for these tests ranged from 3.5 to 5.0 inches with the average depth equal to approximately 4.5 inches. The acceleration data from the first three tests were incomplete, thus only accelerations from tests 4 and 5 were compared with analysis. The peak accelerations for tests 4 and 5 ranged from a low of 16 G's to a high of 19 G's. The penetrometer test accelerations and pulse shapes were first compared with a rigid penetrometer model that was developed using the Mat 5 material model to represent the sand. Pictures of the finite element penetrometer model simulating a 16 ft/s impact into soil are shown in Figure 6.





(a) Model of penetrometer and soil. (b) Model of hemispherical penetrometer.

Figure 6. LS-DYNA hemisphere penetrometer and soil model.

For the Mat 5 model, the dry-sand pressure versus crush factor data, reported in Reference 11, was converted to pressure versus natural strain by calculating  $\ln(1-\text{crush factor})$  as required by the Mat 5 model. Nine data points were entered to capture the entire curve. Since dry sand has no cohesion,  $C$  equals zero, and the shear failure surface has only one non-zero component, which is  $a_2$ . From tri-axial test data for sandy soils [12],  $a_2$  was first estimated to be 0.6. After comparing test with analysis, a value of 0.3 was found to produce better results. The input values for the model are shown in Table 1. The Mat 5 penetrometer model results are compared with test data, as shown in Figure 7. The maximum displacement of the soil using the Mat 5 model is 4.6 inches, which compared well with the average crater depth from the drop tests. A computer graphic illustration of the model showing the crater is illustrated in Figure 8. Gravity is important and was used in all models. Under gravity, the Mat 5 soft soil had to be constrained on the sides to prevent flowing.

Table 1. Mat 5 Input for Soft Soil

Variable	LS-DYNA	Value	Units
Density	RO	1.36E-04	lb-s <sup>2</sup> /in <sup>4</sup>
Shear Modulus	G	267	psi
Bulk Unloading Mod	K	10000.	psi
Yield Surface Coeff	A0	0	psi <sup>2</sup>
Yield Surface Coeff	A1	0	psi
Yield Surface Coeff	A2	0.3	-
Pressure Cutoff	PC	0	psi
Crushing option	VCR	0 (default)	-
Reference Geometry	REF	0 (default)	-

After the Mat 5 sand material model was validated with the penetrometer acceleration and crater depth test data, the pre-test model of the fuselage section was updated (the Mat 63 soil model was replaced with the Mat 5 soil model) and re-executed. No other changes were made to the model. A picture of the model after the simulation is shown in Figure 9. The predicted crater depths left by the DEA are over 8 inches. Recall, the crater depths were measured to be from 7.5 to 9 inches. The model predicted the maximum dynamic crush of the 20-in high DEA to be about 7 inches.

Comparisons of predicted and experimental acceleration, velocity, and displacement responses are shown in Figure 10. The analytical and experimental data were obtained from an accelerometer located on the center right lead block. In general, good correlation was obtained. However, the fuselage acceleration results with the Mat 5 sand material model are only slightly better than the pre-test predictions with Mat 63 [11]. The predicted depth of the crater with the Mat 5 sand model compared very well with the measured depth, whereas in the pre-test model the crater depth was under predicted. Also, the velocity and displacement responses, shown in Figures 10(b) and 10(c) respectively, are closer to the test responses than the pre-test predictions, reported in Reference 11.

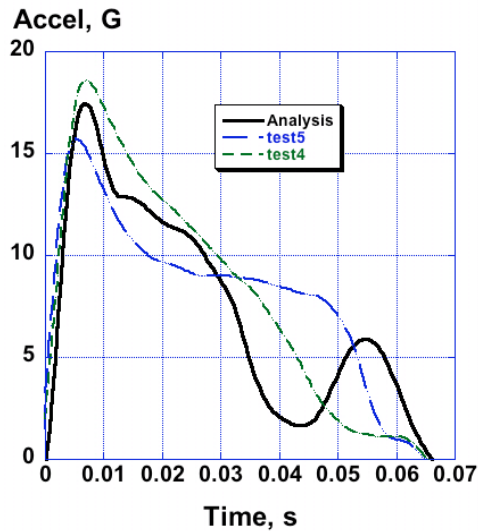


Figure 7. Penetrometer accelerations from tests 4-5 compared with Mat 5 model.



(a) Prior to penetrometer impact. (b) Maximum deformation of sand.

Figure 8. LS-DYNA model of a penetrometer drop into sand.

Several factors may influence the level of test-analysis correlation. First, the unloading bulk modulus was not directly measured, and may be slightly too large for these simulations. A volumetric compression test with unloading is needed to get an experimental value; however, this test was not performed. Finally, it should be noted that the scatter from the penetrometer

tests showed that the sand likely had not stabilized sufficiently to be considered consistent and uniform.

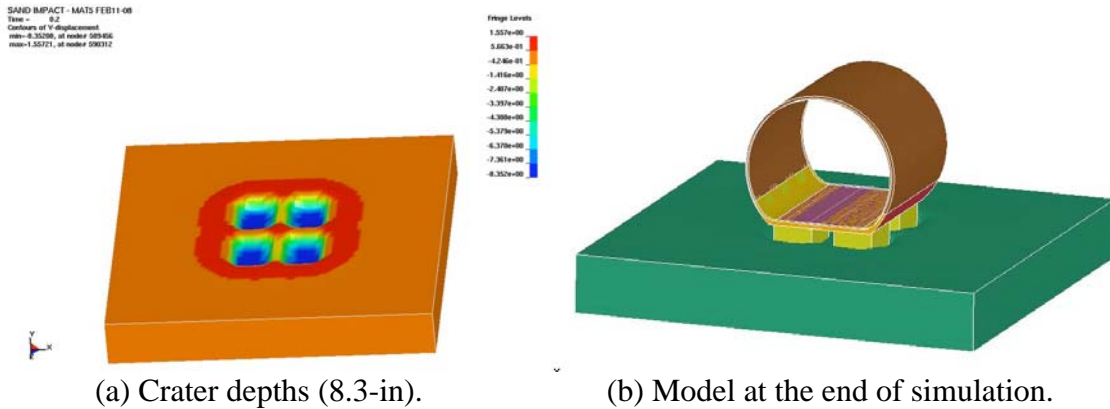


Figure 9. Crater depths of the DEA and the fuselage model at the end of the simulation.

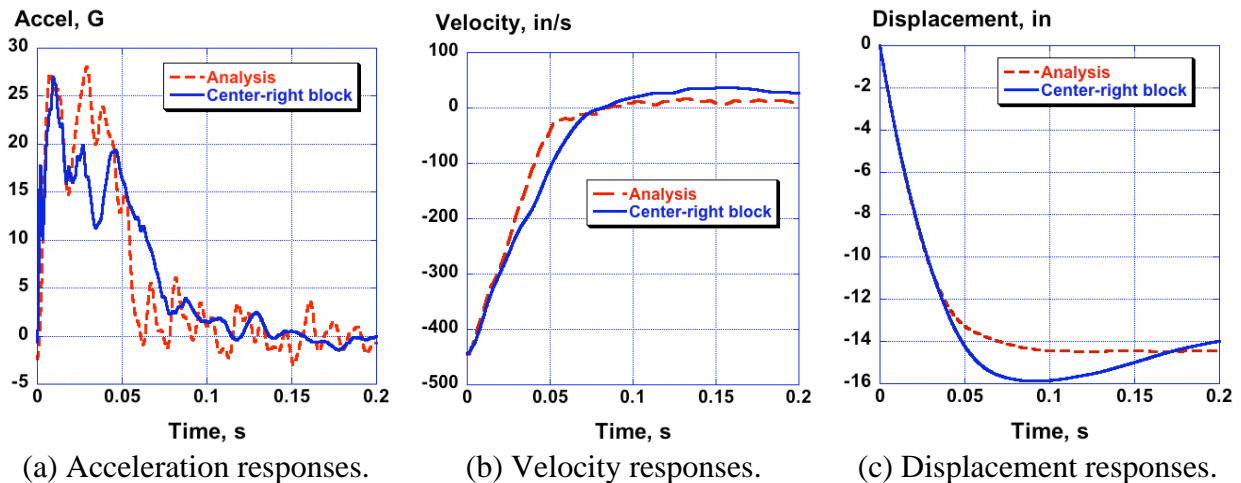


Figure 10. Correlation of LS-DYNA predictions with test data using the Mat 5 material model for the soil.

### *Orion Capsule Impact Tests Onto Gantry “Unwashed Sand” and Simulations*

A 42-ft x 258-ft rectangular soil surface located beneath the gantry at the Landing and Impact Research (LandIR) facility, was impacted by a 4025-lb boilerplate capsule during a series of swing tests, as shown in Figure 11. Note that the LandIR facility, synonymously referred to as the “gantry” in this paper, was formerly known as the Impact Dynamics Research Facility (IDRF) [13]. The two tests that were selected for correlation studies were conducted at a horizontal velocity of 58 ft/s and with a vertical velocity of 5 ft/s. The vertical velocity condition represents the residual velocity after a typical retrorocket burn, and the horizontal velocity represents a scenario in which a very high wind carries the parachute with its capsule. The only difference between the two tests was the pitch angle at impact. In test 19, the capsule was pitched at approximately 0°, and in test 20 the pitch at impact was set to -15°. The soil thickness varied from 2 to 3 feet and was supported by the reinforced concrete test pad at LandIR. The soil was packed, which produced a relatively high density.



Figure 11. Boilerplate swing test at the NASA Langley LandIR facility.

The soil, designated “Unwashed Sand” in Reference 5, was analyzed to determine Mat 5 material properties for input into LS-DYNA computer simulations. The sample was prepared to match a moisture content of 12 percent and a weight density of 130 pounds per-cubic-foot that was approximately the average values measured at LandIR. The Mat 5 model generated for unwashed sand in Reference 5 was used without adjustments in these analyses. The properties for this model are shown in Table 2. For best results, some adjustment of the density, pressure curves, and the shear failure surface should be made to match up with the exact soil conditions at the time of the test. The results of the tri-axial compression tests for the gantry unwashed sand are shown in Figure 12. Note that the soil “flows” both in the radial and axial direction once the shear strength is exceeded for a given confining pressure. The soil strength was determined for five confinement pressures as shown in Figure 12. Using the data in Figure 12, the strength curve is plotted in Figure 13. For example, the red point in Figure 13 has the maximum stress difference of the bottom curve in Figure 12 (10 psi) plotted on the Y-axis and the mean stress on the X-axis. Recall that the mean stress is just twice the confining stress plus the axial stress summed and divided by 3, which gives about 5 psi on the X-axis. From the straight line fit in Figure 13, the a-coefficients of the shear envelope can be calculated using Eq. 4 to be:  $a_0=6.33$ ,  $a_1=3.71$ , and  $a_2=0.543$ . Figure 14 illustrates the compressibility of the soil obtained from the uniaxial strain test and illustrates the 10 points that are input in the Mat 5 material model.

Table 2. Mat 5 input for Gantry “Unwashed Sand.”

Variable	LS-DYNA	Value	Units
Density	RO	1.96E-04	lb-s <sup>2</sup> /in <sup>4</sup>
Shear Modulus	G	3340	psi
Bulk Unloading Mod	K	19370	psi
Yield Surface Coeff	A0	6.326	psi <sup>2</sup>
Yield Surface Coeff	A1	3.707	psi
Yield Surface Coeff	A2	0.543	-
Pressure Cutoff	PC	-1	psi
Crushing option	VCR	0 (default)	-
Reference Geometry	REF	0 (default)	-

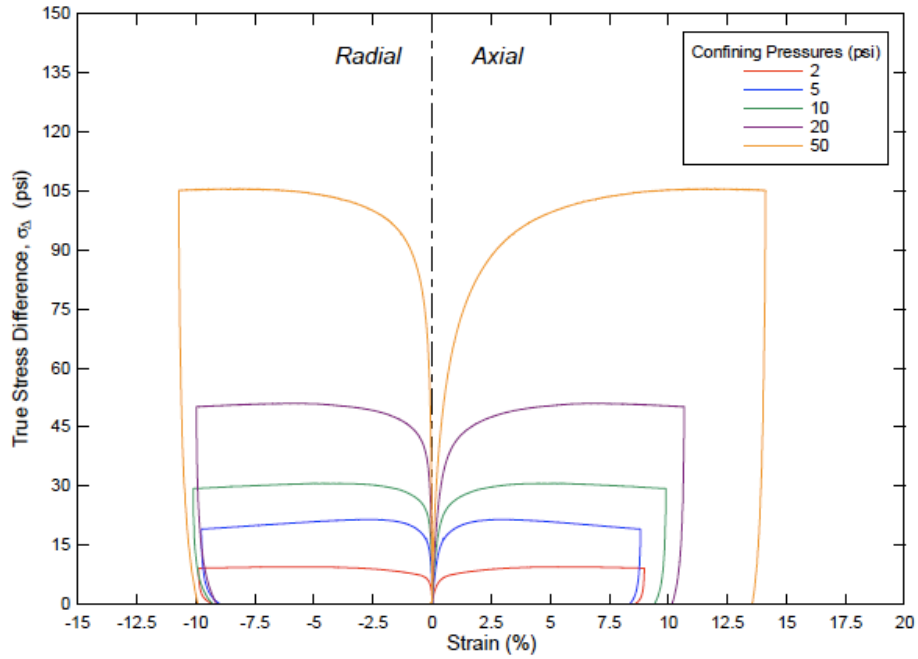


Figure 12. Tri-axial compression test results for the gantry soil (“unwashed sand”).

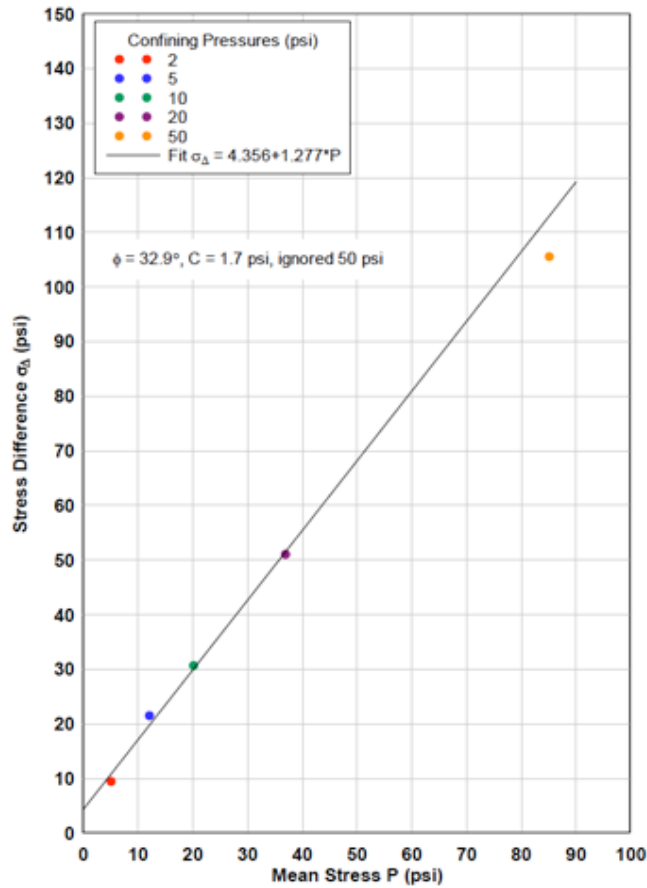


Figure 13. Strength curve for unwashed sand plotted from data in Figure 12.

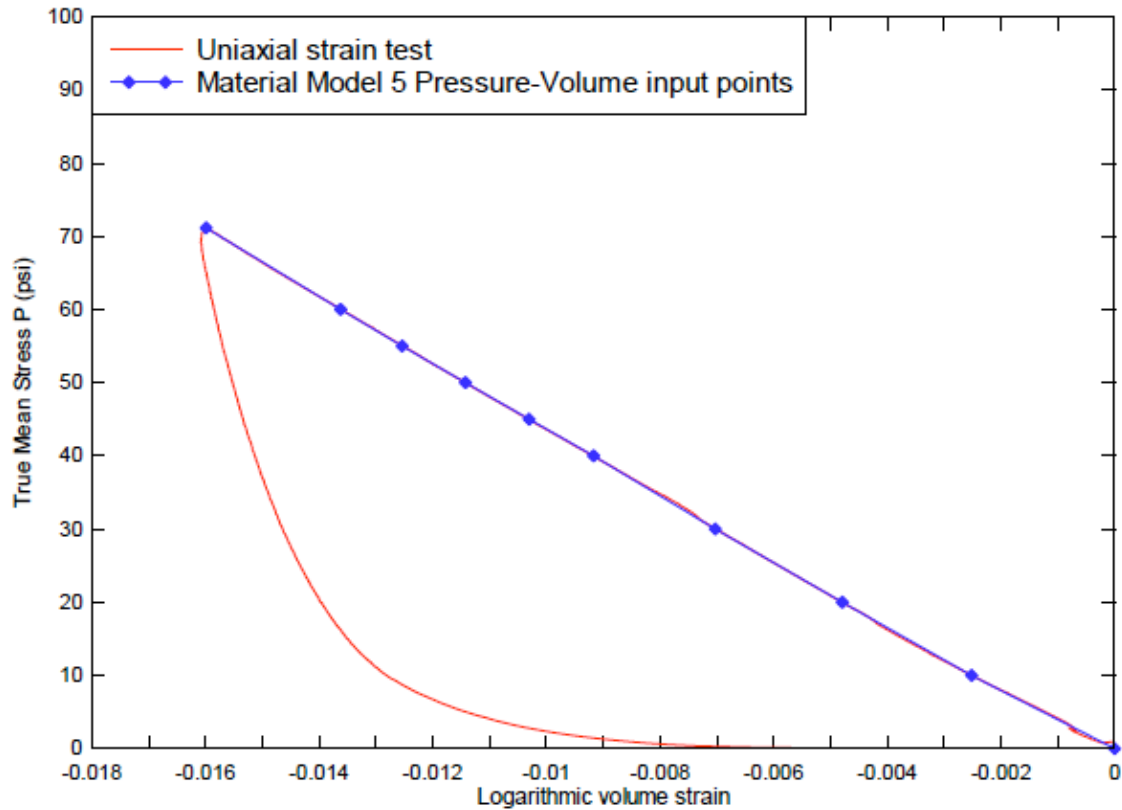


Figure 14. Compressibility (stiffness) for gantry unwashed sand from uniaxial test. The 10 points shown are input into the LS-DYNA model.

A picture of the LS-DYNA model of the scaled boilerplate is shown in Figure 15. The ½-scale boilerplate was modeled as rigid with principal moments of inertia and mass calculated from the test article, but not scaled to Orion. Only the size was scaled. The model is shown in Figure 15 at initial contact between capsule and soil for the  $-15^\circ$  pitch impact. The horizontal velocity vector of the boilerplate at soil contact points in the  $-Y$  global direction (from left to right). The boilerplate is modeled as a rigid body with  $I_{y'y'} = 8160 \text{ lb-in-sec}^2$ ,  $I_{x'x'} = 10000 \text{ lb-in-sec}^2$ , and  $I_{zz} = 10160 \text{ lb-in-sec}^2$ , about the vehicle local coordinate system. The soil domain is numerically modeled as a homogeneous material 200 ft. long, 20 ft. wide, and 1.5 ft. deep. The soil domain is discretized using constant 4 in. x 4 in. x 4.5 in. brick elements. Zero translation and zero rotation boundary conditions are enforced along the sides and base of the soil.

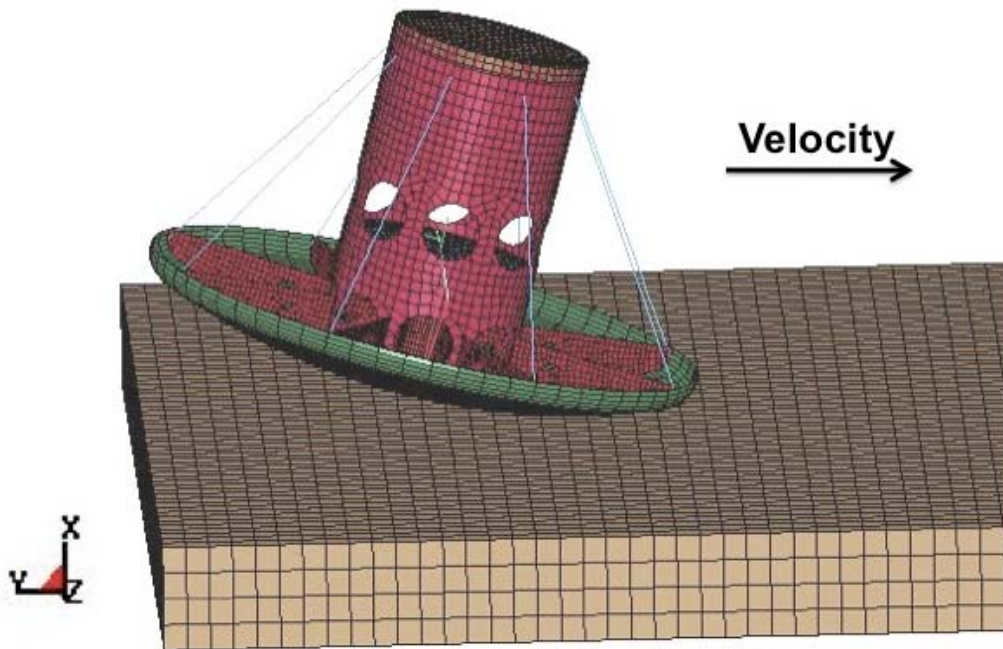


Figure 15. Finite element model of the rigid boilerplate pitched down at  $-15^\circ$ .

The boilerplate skidded approximately 96 ft for the  $0^\circ$  pitch attitude and 97 feet for the  $-15^\circ$  pitch attitude before coming to rest. One objective in developing computer simulations for the swing tests was to determine the sliding friction coefficient at the soil-boilerplate interface. The forces due to sliding friction and the forces due to moving soil (plowing) are difficult to separate. The horizontal force required to pull the capsule at constant velocity over the soil, if divided by the weight of the capsule, would imply that the friction coefficient is approximately 0.6. However, for all but the hardest soils, some plowing occurs. The stopping distance cannot be used in a simple calculation to determine the friction coefficient since the capsule skips over the soil instead of making constant contact. Consequently, the friction coefficient is varied in LS-DYNA and the computed stopping distance is compared with test in Figure 16. From Figure 16, the stopping distance versus friction behavior can be approximated as a second-order polynomial. Based on a stopping distance of 96- and 97-feet for the two tests, the average coefficient of friction between the boilerplate and soil is 0.45. In comparison, a block sliding with an initial velocity of 58-ft/s on a solid smooth surface with a 0.45 friction coefficient stops in 116 ft. The difference in the two stopping distances implies the significance of plowing while the boilerplate traverses the soils.

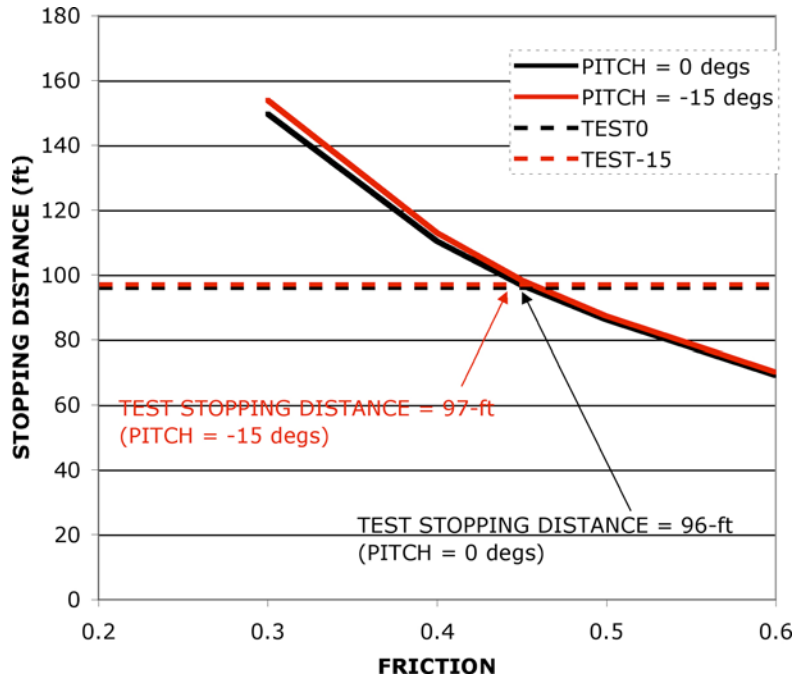


Figure 16. Stopping distance for two boilerplate swing tests versus contact friction coefficient computed from LS-DYNA model.

LS-DYNA predicted horizontal and vertical accelerations at the boilerplate center of gravity are compared with the  $-15^\circ$  pitch experimental accelerations in Figures 17 and 18, respectively. Only the first two seconds of the time histories are shown for clarity. Comparisons of test and analysis acceleration time histories are shown in the vehicle local coordinate system. A 0.45 friction coefficient was used for the computer simulations to match the slide out distance. To remove high frequency vibrations, which obscure the low frequency impact data, acceleration time histories from the boilerplate were filtered using an SAE CFC60 filter [14]. The test data and the simulation show acceleration peaks that are of similar magnitude. However, the unevenness of the soil perturbs the acceleration frequency and magnitude in the test. The LS-DYNA simulation shows 13 separate “skips” or impacts during the two-second interval. The experimental data shows either 13 or 14 peaks depending on how one interprets the small impacts between 1.2 and 1.4 seconds. Note in Figure 18, when the boilerplate is rebounding following an impact, it is free falling with  $-1g$  acceleration. At the same time, while airborne, the boilerplate experiences 0 horizontal deceleration, as shown in Figure 17. The LS-DYNA simulation animation compares quite well with the high-speed videos for both of these tests. The  $0^\circ$  pitch case is similar, but is not shown.



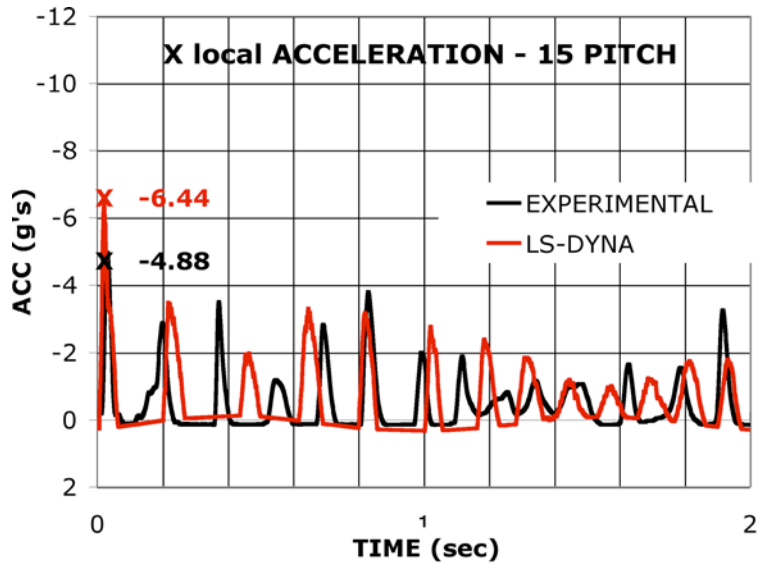


Figure 17. Comparison of horizontal accelerations for soil impact for the  $-15^\circ$  pitch case.

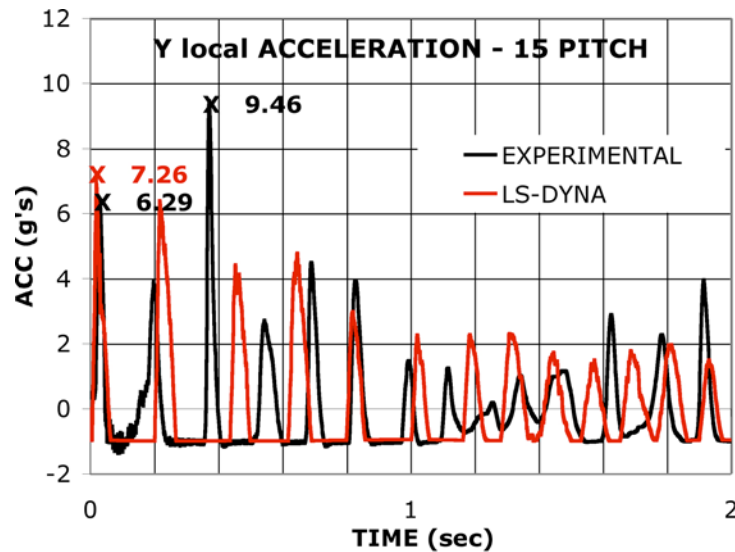


Figure 18. Comparison of vertical accelerations for soil impact for the  $-15^\circ$  pitch case.

Vertical drop tests of the boilerplate capsule onto soil were performed using the vertical drop tower at LandIR onto level and sloped gantry soil surfaces, as shown in Figure 19. The contained level soil in Figure 19 was 48-in deep and was scooped from the “unwashed sand” material that was used as the impact surface during the swing tests. The first test was a drop at 12-ft/s and a second test was conducted at 24 ft/s, both with zero pitch. The Mat 5 soil model was the same as used in the swing test as shown in Table 2. Each brick element of soil in the model was 4x4x4-in. A comparison of tests 1 at 12 ft/s and test 2 at 24 ft/s with analyses is shown in Figure 20. The model and test data initially load along the same slope, but then deviate. The peak accelerations predicted by LS-DYNA were slightly higher for both cases. For both tests, the test acceleration decay time was longer than that predicted by analysis. Both test

and analysis for these cases were filtered with a Butterworth 60 Hz low-pass digital filter, which should not be confused with an SAE class-60 filter.

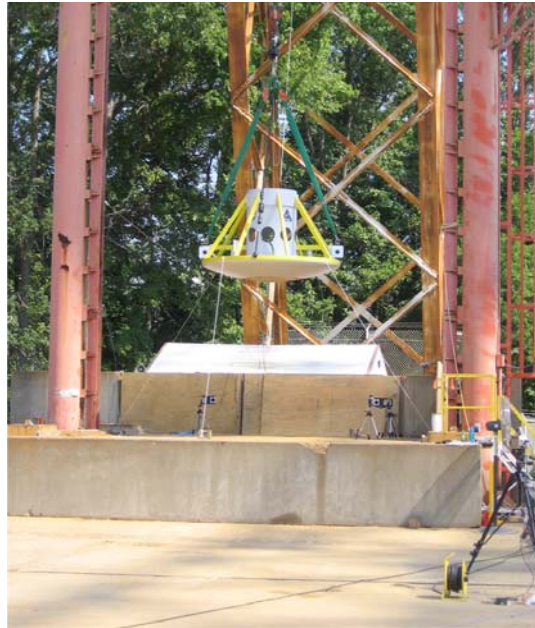


Figure 19. First vertical drop test of boilerplate into flat soil impact surface using the vertical drop tower at LandIR.

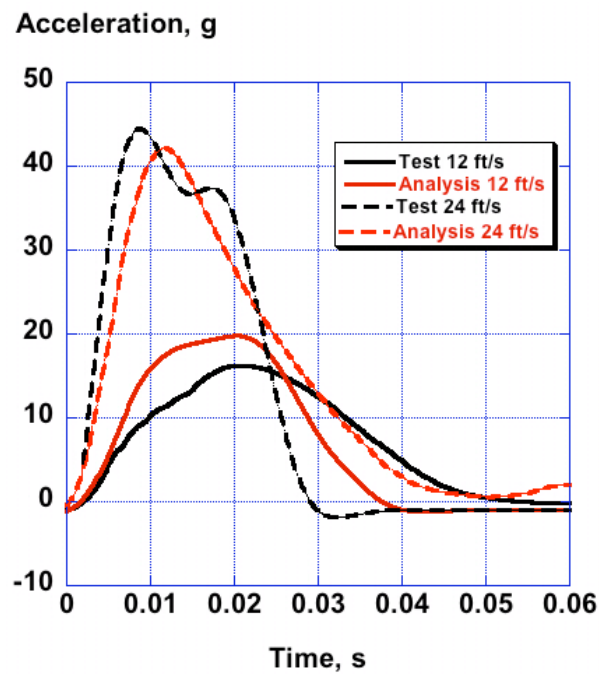


Figure 20. Comparison of model with vertical CG-acceleration for boilerplate vertical drop tests at 12 ft/s and 24 ft/s.

Finally, a study was performed to determine the sensitivity of the Mat 5 input on the resulting acceleration peak of the boilerplate capsule for the 24-ft/s vertical drop case. This sensitivity study is valid only for the condition studied. Since each parameter is varied  $\pm 20\%$ , this study does not take into account the parameter variances. Results of the study are shown in Figure 21, indicating that the input properties that are most important for this particular analysis are, in the following order: 1) density, 2) the compressibility or stiffness, which is input via the volumetric strain versus pressure, and 3) the shear strength parameter  $a_2$ . Note that moisture content generally lowers the shear strength and must be known along with the density before an accurate model can be generated. Also, the soil must be uniform with respect to compaction (density), particulate size, and moisture content. Often, in-situ soil is quite variable from location to location.

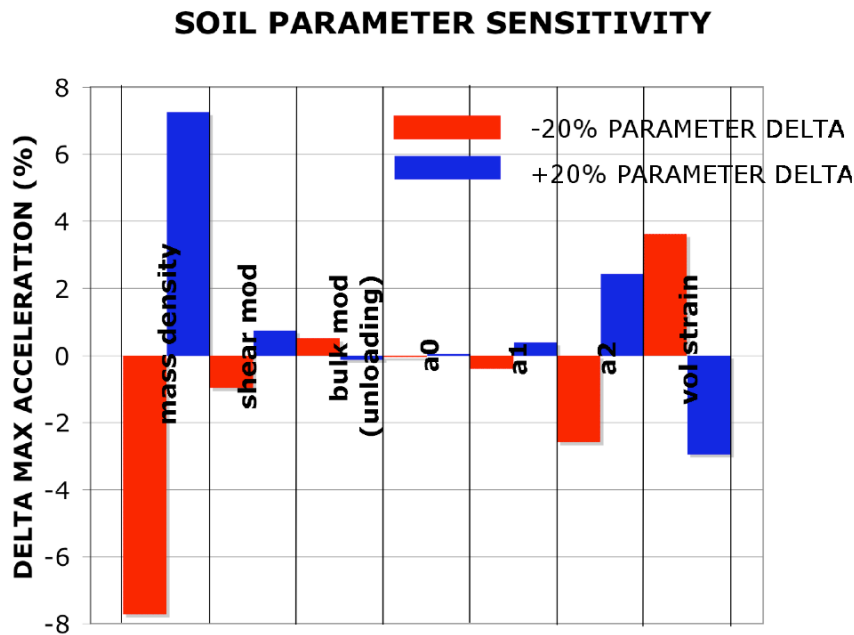


Figure 21. Mat 5 soil parameter sensitivity study.

### Concluding Remarks

This paper describes fundamental soils characterization work performed at NASA Langley Research Center in support of the Subsonic Rotary Wing Aeronautics Program and the Orion Landing System Advanced Development Program. LS-DYNA soil impact model development and test-analysis correlation results were presented for: (1) a 38-ft/s vertical drop test of a composite fuselage section, outfitted with four blocks of deployable energy absorbers, onto sand, and (2) a series of impact tests of a  $\frac{1}{2}$ -scale geometric boilerplate Orion capsule onto soil. The LS-DYNA model showed good correlation with the 38-ft/s drop test into sand. After calibration using drop tests of an instrumented hemispherical penetrometer, the Mat 5 material model

provided a good representation of the unpacked sand. The fuselage acceleration, the energy absorber stroke, and the depth of the crater in the sand were all well captured.

Reasonable results were obtained with the Mat 5 material model for Orion boilerplate impacts onto the “unwashed gantry sand,” which is a sand and clay mix. Although a single sample of the “unwashed gantry sand” was characterized in a soils testing laboratory, the in-situ soil material properties for a given impact test at LandIR could vary considerably depending on the inhomogeneity of the soil from location to location, soil density variations with depth (packing), moisture content variations, and other ambient conditions. The boilerplate model impacting onto the “unwashed gantry sand” relied on input from a soils laboratory to generate parameters for Mat 5. The predicted peak accelerations of the model were relatively close to measured values. A dynamic friction coefficient was determined by executing LS-DYNA models of the Orion boilerplate with different friction coefficients and comparing analysis with experimental slide-out distances. From this study, the best friction coefficient for use in LS-DYNA on the contact card was estimated to be approximately 0.45. The pull force divided by the weight of the boilerplate for a slow constant velocity would imply a friction coefficient of 0.6. However, the soil was also being sheared and plowed in those tests. Finally, a simple sensitivity study of Mat 5 parameters was conducted for a 24-ft/s vertical drop test of the ½-scale boilerplate onto the “unwashed gantry sand.” The Mat 5 parameters that influenced the boilerplate peak acceleration most were the soil density and the volumetric strain versus pressure (compressibility).

## References

1. Jackson, K.E., Fuchs, Y. T., and Kellas, S., “Overview of the NASA Subsonic Rotary Wing Aeronautics Research Program in Rotorcraft Crashworthiness,” Proceedings of the 11<sup>th</sup>ASCE Earth and Space Conference, Special Symposium on Ballistic Impact and Crashworthiness of Aerospace Structures, Long Beach, CA, March 3-5, 2008.
2. Fasanella, Edwin L., “Multi-Terrain Earth Landing Systems Applicable for Manned Space Capsules.” Proceedings of the 11<sup>th</sup>ASCE Earth and Space Conference, Special Symposium on Ballistic Impact and Crashworthiness of Aerospace Structures, Long Beach, CA, March 3-5, 2008.
3. Hallquist, John O., “LS-DYNA Keyword User’s Manual,” Version 971, Livermore Software Technology Company, Livermore, CA, August 2006.
4. Thomas, Michael A. et. al., “Constitutive Soil Properties for Cuddeback Lake, CA and Carson Sink, NV,” Applied Research Associates, Inc., NASA CR-2008-215345, August 2008.
5. Thomas, Michael A. et. al, “Constitutive Soil Properties for Unwashed Sand and Kennedy Space Center,” Applied Research Associates, Inc., NASA CR-2008-215334, July 2008.
6. Thomas, Michael A. et. al., “Constitutive Properties for Clean Sand at Langley Gantry Facility,” Applied Research Associates, Inc., May 2008 (letter report)

7. Hallquist, John O., "LS-DYNA Theory Manual," Version 971, Livermore Software Technology Company, Livermore, CA, August 2006.
8. Jackson, K. E., "Impact Testing and Simulation of a Crashworthy Composite Fuselage Concept," *International Journal of Crashworthiness*, 2001, Vol. 6, No 1, pp.107-121.
9. Kellas, S. and Jackson, K., "Deployable System for Crash-Load Attenuation," Proceedings of the 63<sup>rd</sup> American Helicopter Society (AHS) Forum, VA Beach, May 1-3, 2007.
10. Kellas, S. and Jackson, K., "Multi-Terrain Vertical Drop Tests of a Composite Fuselage Section," Proceedings of the 64<sup>th</sup> American Helicopter Society (AHS) Annual Forum, Montreal, Canada, April 29-May 1, 2008.
11. Fasanella, E. L., Jackson, K. E., and Kellas, S., "Soft Soil Impact Testing and Simulation of Aerospace Structures," Proceedings of the 10<sup>th</sup> LS-DYNA Users Conference, Dearborn, MI, June 8-10, 2008.
12. Schwer, Leonard, "Geomaterial Modeling," Class notes and personal communications, Schwer Engineering and Consulting Services, December 2006.
13. Jackson, K. E., Boitnott, R. L., Fasanella, E. L., Jones, L.E., and Lyle, K. H., "A Summary of DOD-Sponsored Research Performed at NASA Langley's Impact Dynamics Research Facility (IDRF)," *Journal of the American Helicopter Society*, Vol. 51, No.1, January 2006, pp 59-69.
14. Society of Automotive Engineers (SAE), Recommended Practice: Instrumentation for Impact Test – Part 1, Electronic Instrumentation, SAE J211/1, March 1995.